Available online at www.sciencedirect.com
SCIENCE DIRECT®
J. Anal. Appl. Pyrolysis 71 (2004) 353–374
JOURNAL of ANALYTICAL and APPLIED PYROLYSIS
www.elsevier.com/locate/jaap

Development of a semi-empirical model for pyrolysis of an annular sawdust bed

M.R. Ravi*, Anurag Jhalani, Sanjiv Sinha, Anjan Ray

Department of Mechanical Engineering, Indian Institute of Technology, New Delhi 110016 India

Received 22 November 2001; accepted 29 May 2003

Abstract

A model for simulating pyrolysis of sawdust in a packed bed of annular shape has been developed. Heat transfer is assumed to be purely due to conduction, and chemical reaction of pyrolysis has been approximated to a pseudo-first order reaction. The reaction rate constant has been obtained as a function of temperature for the species of sawdust used in the present work using thermogravimetric analysis, and its variation with heating rate has been accounted for. Thermal conductivity of the packed bed of sawdust has been estimated experimentally by temperature measurement in the sawdust bed. The sawdust bed was pyrolysed using an electric heater in contact with the inner surface of the annulus as the source of energy. Using the history of temperature profiles measured on the heater wall at various points of time, a simulation of the experiment has been carried out. The predicted mass loss history compares reasonably well with the measured one. A sensitivity analysis using the model suggests that the predictions may be improved by considering the flow of volatiles in the void space of char bed, and by accounting for secondary pyrolysis due to residence of volatiles in the bed.
© 2003 Elsevier B.V. All rights reserved.

Keywords: Pyrolysis; Sawdust bed; Modelling; First-order kinetics; Porous medium

1. Introduction

Pyrolysis, the process of thermochemical decomposition of fuels, is a complex phenomenon, primarily due to the sheer range and number of chemical reactions that comprise it. It forms an important step in the combustion of biomass fuels such as wood. Since it is the products of pyrolysis, namely, char and volatiles, that later undergo combustion to release

* Corresponding author.
E-mail address: ravimr@mech.iitd.ac.in (M.R. Ravi).

0165-2370/$ – see front matter © 2003 Elsevier B.V. All rights reserved.
doi:10.1016/S0165-2370(03)00102-5

Nomenclature

A	apparent pre-exponential factor
C_p	specific heat
E	apparent activation energy
f	volume fraction
k	thermal conductivity
k_r	Arrhenius rate of apparent first order reaction
m	mass
q	heat flux
$\dot{Q}_{heater}$	input power to sawdust bed from heater
r	radial coordinate
$\Re$	universal gas constant
R_{th}	thermal resistance
ρ	density
t	time coordinate
T	temperature
U	overall heat transfer coefficient
V	volume
z	axial coordinate

Subscripts

∞	value pertaining to completely pyrolysed sawdust
amb	ambient
ch	char
sd	sawdust
w	heater wall, moisture

energy, a mathematical model of pyrolysis provides a useful tool to study combustion. The powdered form of wood, commonly referred to as sawdust, finds widespread use as a fuel for cookstoves, especially among the third world population. Since sawdust has the same chemical composition as wood, the chemical reactions during pyrolysis may be expected to be the same in both the cases. However, the dynamics of pyrolysis are different for wood and sawdust, due to the differences in physical structure.

In this paper a model for pyrolysis in a packed bed of sawdust has been presented. The bed considered for the present study has the shape of a cylindrical annulus. Such annular packing of sawdust is typical to cookstoves that use sawdust as fuel. The cross-section of a typical sawdust stove is shown in Fig. 1a. It has an L-shaped hole in a bed of packed sawdust. The stove is lit using a flame source inserted through the horizontal leg of the L-shaped passage. When the stove is lit, the hot gases in the flame heat up the sawdust on the inner surface of the passage. This sets up a pyrolysis wave that travels outwards into the annular bed, emitting the volatile matter into the flow passage. The combustion of these volatiles sustains further pyrolysis. The air required for combustion enters from the bottom of the

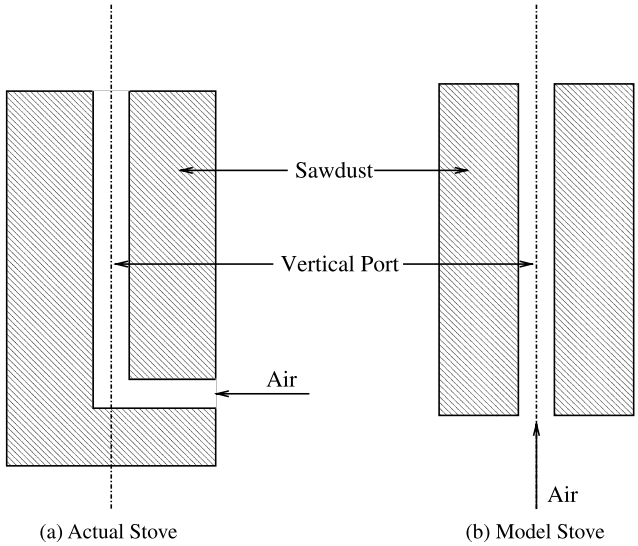

Fig. 1. Schematic of a sawdust stove.

passage, due to buoyancy caused by the rising hot gases from the flame. Thus, combustion, pyrolysis and natural convection sustain each other in a symbiotic phenomenon.

The combustion of volatiles in the central passage of the stove provides the heat energy required to initiate pyrolysis. The mechanism of pyrolysis involves heat transfer from the hot flame zone into the sawdust bed, the thermochemical decomposition of sawdust into char and volatiles, and the flow of the volatiles into the flame zone from the sawdust bed. Owing to the escape of volatiles the porosity of the solid bed increases continuously resulting in an enhancement in the flow of volatiles inside the bed. This increase in porosity and the formation of char result in continual change of properties of the bed, namely, density, thermal conductivity and specific heat.

Thermochemical decomposition of wood, which is constituted by cellulose, hemicellulose and lignin, is complex by virtue of the hundreds of chemical reactions involved in the process. The residence of volatiles in a zone being pyrolysed is known to catalyse pyrolytic decomposition, resulting in an increase in the rate of pyrolysis. For the sake of modelling, it is often simplified using apparent chemistry schemes involving a single-step reaction, parallel single-step reactions or a sequence of simple reactions. A comprehensive review on the phenomenon of pyrolysis can be found in Zaror and Pyle [1].

Attempts to model pyrolysis of wood, the most widely used fuel in the world, began with the pioneering work of Bamford et al. [2], whose model used a single reaction scheme, first order kinetics and heat conduction equation. Thereafter, several models have been developed which have considered diverse issues in wood pyrolysis. Internal convection between solid wood and volatiles was modelled by Kung [3], Matsumoto [4], Maa and Bailie [5], and Roberts [6]. The effect of char formation was considered by Kung [3], and the rate of char removal by oxidation was modelled by Matsumoto [4]. Temperature-dependent property variation was accounted for by Kung [3], Matsumoto [4], Maa and Bailie [5], Kansa et al.

[7] and Chan et al. [8]. Multi-step reaction schemes have been presented by Tinney [9], Kung [3], Chan et al. [8] and Koufopanos et al. [10]. Issues related to heat of reaction of pyrolysis have been modelled by Lee et al. [11], while the effect of anisotropy of the pyrolysing medium has been accounted for by Kansa et al. [7]. Combined heat and mass transfer with Darcian flow of volatiles through the porous matrix of pyrolysing medium has been accounted for by Di Blasi [12]. Detailed reviews on modelling of pyrolysis can be found in Di Blasi [13] and Sinha et al. [14].

It has been found from available literature that the data on pyrolysis reaction rates of wood span a wide range of values, since the data depend on a multitude of factors such as the species of wood, its moisture content, size of the sample, rate of heating, etc. Therefore, it is essential to make one's own measurements if one needs to reliably validate one's model. Few papers are available which support their models with their own experimental results [17]. Besides, all the work carried out on pyrolysis of sawdust has been on small samples, and work on larger samples has primarily been on blocks of wood. Issues such as variation of bulk thermal conductivity with porosity of the pyrolysing bed have not been investigated in literature for sawdust.

In this paper, a model for pyrolysis has been developed for the geometry of sawdust stove simplified as shown in Fig. 1b. In the model stove, heat source for pyrolysis is an electric heater instead of the flame, enabling decoupling of pyrolysis from combustion. A single-step reaction scheme has been chosen, and the apparent rate constant as a function of temperature has been obtained experimentally using thermogravimetric analysis (TGA). Variation of the rate constant with heating rate has been accounted for. Heat transfer in the annular sawdust bed has been assumed to be purely due to conduction. Thermal conductivity of virgin sawdust for use in the model has been estimated from temperature measurements in the bed. The model predictions of mass loss due to pyrolysis for the values of measured heater wall temperatures have then been compared with experimentally measured mass loss histories. A sensitivity analysis has been conducted using the model to study the effects of the uncertainties in physical property data and rate constants on the mass loss histories predicted by the model.

2. Formulation of the model

The overall model for pyrolysis may be broken down into the sub-models of heat transfer and chemical kinetics. Modelling of pyrolysis in a sawdust bed though similar to wood pyrolysis, differs in some respects. Anisotropy, a major issue in wood pyrolysis is non-existent for the present case. However, porosity of the bed influences pyrolysis greatly in the present context. Autocatalytic secondary pyrolysis reactions may also be expected to occur due to large residence time of volatiles inside the bed. While the present model accounts for the changing porosity of the bed by variable properties, it does not consider the residence time of volatiles, i.e., secondary pyrolysis reactions have been ignored for the sake of simplicity. In the present work a single-step apparent kinetics scheme for pyrolysis has been used. Reaction rates obtained using TGA at heating rates of 10 and 100 $^{\circ}$C min^{-1} have been used to compute the reaction rates at the heating rates encountered in the sawdust bed. It is also assumed that the sawdust bed does not collapse during pyrolysis, i.e., its volume is taken

to be fixed. Heat transfer is assumed to be only by conduction. Heat of pyrolysis has been neglected, since for slow pyrolysis it is known from literature that heat of pyrolysis is small [11]. The latent heat of vaporisation of moisture has been neglected. The following paragraphs present the formulation of the different aspects of the model, and the assumptions made therein.

2.1. Geometry

The L-hole in the actual sawdust stove makes the geometry of the sawdust bed three-dimensional. For simplicity in modelling, the horizontal leg of the passage can be removed to obtain an annular bed of sawdust, which is an axisymmetric geometry as shown in Fig. 1b. The present work considers this annular sawdust bed as a simplified representative of the sawdust stove. An experimental analogue of the sawdust stove of the configuration shown in Fig. 1b was constructed to study the phenomenon of pyrolysis. For this purpose, an electric heater was used as the source of heat for pyrolysis. In the present work, a solid cylindrical heater was completely buried in the bed of sawdust, so that all the heat generated by the heater is supplied to the sawdust for pyrolysis.

2.2. Heat transfer model

The model assumes heat transfer to occur purely by conduction. Flow of volatiles and the resulting convective heat transfer between the volatiles and the bed has been ignored. Shrinkage of the bed and structural effects have been assumed to be absent. It has been assumed that the volume of the sawdust bed remains unaltered due to pyrolysis. The mass loss is assumed to cause a change only in the porosity of the bed, and the variation in thermal conductivity of the bed owing to this change in porosity has been taken into account. At any point inside the bed, the equation of heat transfer is:

$$\frac{1}{r}\frac{\partial}{\partial r}\left(kr\frac{\partial T}{\partial r}\right)+\frac{\partial}{\partial z}\left(k\frac{\partial T}{\partial z}\right)=\rho C_{\mathrm{p}}\frac{\partial T}{\partial t} \tag{1}$$

where ρ, k and C_{p} are the density, thermal conductivity and specific heat of the bed, respectively and T is the temperature of the bed at time t at any point (r, z). The density accounts for the mass lost from each point in the domain. Thermal conductivity of the bed is computed from of those of virgin sawdust, char, moisture and void fractions at any point. Latent heat term due to loss of moisture at any point has been neglected. Treatment of property variation is discussed in detail in Section 2.4.

2.3. Chemical kinetics model

The actual reaction scheme of the pyrolysis of wood is extremely complex because of the formation of over a hundred intermediate products (Shafizadeh [15], Emmons and Atreya [16]). Pyrolysis is therefore generally modelled on the basis of apparent kinetics. Zaror and Pyle [1] suggest a single pseudo-first order reaction scheme. Bilbao et al. [17] have achieved good agreement between the predicted results and experimental data in studies on pyrolysis

of small quantities of sawdust using a first order single reaction scheme. Such a scheme has also been used for the present model, using the following apparent kinetics equation:

$$\frac{\partial \rho}{\partial t} = -k_r\,(\rho - \rho_\infty) \tag{2}$$

where ρ is the bulk density of the bed at any point, defined as the mass of solid matter (sawdust + char) per unit volume of the bed, and ρ_∞ is the density of the bed when pyrolysis gets completed. k_r is the reaction rate of the apparent first order reaction, and it is a function of temperature, heating rate, residence time of volatiles in the bed, etc. In the present work, the effect of residence time of volatiles in the bed has not been accounted for. The values of k_r as a function of temperature were obtained from the TGA on a sample of the sawdust at heating rates of 10 and 100 °C min^{-1}. These rates were then used to compute the k_r values at the heating rates encountered in the sawdust bed. The details of how k_r was obtained from TGA are presented in detail in Section 3.2.

2.4. Variable properties

In the present model, the sawdust bed is divided into several small control volumes, and Eq. (1) has been applied to compute the temperature of each control volume. The properties, viz., thermal conductivity k, density ρ and the specific heat capacity C_p in Eq. (1) change during drying and pyrolysis, primarily owing to the change in the composition and density of the bed. We may suppose that the bed is made up of dry sawdust, moisture, char and void, whose proportions vary as the bed is heated.

Initially, the bed can be supposed to be composed of dry sawdust and moisture alone. At any point, as the temperature rises, the sawdust first loses its moisture, to become dry sawdust. On further increase in temperature beyond 200 °C, pyrolysis begins, and the dry sawdust decomposes into volatiles and char. As the volatiles escape, the bed that remains is made up of char and void. Based on experimental observations, it has been assumed that the sawdust bed retains its volume, i.e., it does not collapse during the progress of pyrolysis. This implies that in any control volume, the loss of mass of moisture and volatiles directly translates into the corresponding volume of void space being created in the control volume. The mass loss at temperatures below 200 °C is entirely owing to drying, and that above 200 °C is almost entirely due to pyrolysis, since most of the moisture leaves the bed by the time its temperature rises to this value.

During drying, the moist sawdust gets converted into dry sawdust. The moisture content of the sample is known from proximate analysis (Table 1). On pyrolysis, i.e., when the temperature in the control volume exceeds 200 °C, sawdust liberates volatiles. The fraction of mass that remains as char is assumed to be equal to the sum of fixed carbon and ash fractions of the proximate analysis presented in Table 1. From TGA, the apparent reaction

Table 1
Proximate analysis of sawdust (as-received basis)

Components	Volatile matter	Fixed carbon	Ash	Moisture
%	70.2	18.9	3.0	7.9

rate k_r (Eq. (2)) has been obtained (cf. Section 3.2) for the entire temperature range covering both drying and pyrolysis, and is used to compute the density change of each control volume at the local temperature. The mass loss from a control volume is then obtained by multiplying the change in density by the volume of the control volume.

As mentioned above, the bed is assumed to be composed of sawdust, char, moisture and void, whose proportions vary with the progress of drying and pyrolysis. For the sake of modelling, the void present in the sawdust bed is not considered separately. Instead, sawdust is treated as a combination of dry sawdust and moisture, with its properties equal to those of the unpyrolysed virgin sawdust bed at its initial packing density. The proportion of each of the constituents in a control volume is computed in terms of the volumetric fraction f occupied by the constituent. Here, f_{sd}, f_w, f_{void} and f_{ch} are the volumetric fractions of sawdust, moisture, void and char, respectively, i.e.,

$$f_{sd} = \frac{\text{Actual volume of sawdust in the control volume}}{\text{Total volume of the control volume}}$$

and f_{ch}, f_w and f_{void} are defined in a similar manner. The actual volume of each constituent in the control volume is obtained by dividing the mass of the constituent in the control volume at that time by its respective density. While f_{sd}, f_{ch} and f_w are obtained using the above relation, f_{void} is computed by subtracting the sum of the other fractions from unity:

$$f_{void} = 1 - f_{sd} - f_{ch} - f_w$$

The properties of the bed in each control volume are now defined in terms of the properties of the four constituents and their volumetric fractions, as described below.

The local density ρ is defined in terms of the volumetric fractions of sawdust, moisture and char as

$$\rho = \rho_{sd} f_{sd} + \rho_{ch} f_{ch} + \rho_w f_w \tag{3}$$

The mass of the gases in the void space has not been considered in the evaluation of density. Density of moist sawdust has been measured experimentally to be 230 kg m^{-3}. The solid matter in the char bed is predominantly carbon, and its properties can be reasonably assumed to be the same as those of graphite [21]. Thus, the density of solid char has been taken to be that of graphite [20].

Thermal conductivity of a packed sawdust bed of the kind used for the present work can be approximated by

$$k = k_{sd}^{f_{sd}} k_{ch}^{f_{ch}} k_w^{f_w} k_{void}^{f_{void}} \tag{4}$$

where k_{sd} and k_{ch} are the thermal conductivities of sawdust and char, respectively, and k_{void} is that of the fluid in the void [19]. Moisture is assumed to be present in the bed in the form of liquid water, and thus, ρ_w and k_w are taken to be the density and conductivity of liquid water. Thermal conductivity of sawdust sample used in the present work at its packing density of interest was determined by experiment as part of the present work (cf. Section 3.1). Since the sawdust sample included moisture, the thermal conductivity of dry sawdust, k_{sd}, is computed from this data using Eq. (4), as described in Section 3.1. The solid char and void space in the char bed are separately accounted for in Eq. (4) for computation

Table 2
Physical properties used in the simulation model

Property	k (W m^{-1} K^{-1})	ρ (kg m^{-3})	C_p (kJ Kg^{-1}K^{-1})
Sawdust	Table 3	230	Eqs. (5a) and (5b)
Char	2.68	2210	Eq. (5c)
Void	0.0456	–	–
Moisture	0.675	985	4.197

of thermal conductivity of the bed. Thermal conductivity k_{ch} of solid char is taken to be that of graphite across the grains [20]. For void, k_{void} is taken to be that of air at 600 K.

Specific heat of char and sawdust do not vary with porosity. Specific heat of sawdust, which is the same as that of wood, depends on the moisture content and temperature, and has been accounted for using the following expressions [21]:

$$C_{p,\text{dry-wood}} = 0.1031 + 0.003867T \ \text{kJ (kg K)}^{-1} \tag{5a}$$

$$C_{p,\text{wet-wood}} = \frac{\left(C_{p,\text{dry-wood}} + 4.187M\right)}{1+M} + (0.02355T - 1.32M - 6.191)M \ \text{kJ (kg K)}^{-1} \tag{5b}$$

where M is the mass fraction of moisture in the sawdust at any point at a given instant and T is the absolute temperature. Specific heat of char can be assumed to be that of graphite [21], and its variation with temperature has been accounted for, as given by Butland and Maddison [22], for a temperature range of 250–3000 K:

$$C_{p,ch} = 4.187 \times \left(0.538637 + 9.11129 \times 10^{-6}T - \frac{90.2725}{T} - \frac{43449.3}{T^2} + \frac{1.59309 \times 10^7}{T^3} - \frac{1.43688 \times 10^9}{T^4}\right) \ \text{kJ (kg K)}^{-1} \tag{5c}$$

The mean specific heat of each control volume can then be written as a mass-weighted average of its constituent specific heats, neglecting the heat capacity of void, as

$$C_p = \frac{\rho_{sd} f_{sd} C_{p,sd} + \rho_{ch} f_{ch} C_{p,ch} + \rho_w f_w C_{p,w}}{\rho_{sd} f_{sd} + \rho_{ch} f_{ch} + \rho_w f_w} \tag{6}$$

The values of k, ρ and C_p of sawdust and char used in the present work are summarised in Table 2.

2.5. Solution methodology

The domain of interest for the present work is the annular bed of sawdust, whose dimensions are the same as those in the experimental set-up presented in Section 4.1. It is discretised using 17×61 grids in the r and z directions, respectively on the axisymmetric plane, with non-uniform spacing in r direction. Since sawdust particles of size of the order of 1 mm have been used in the present study, the minimum size of grid control volumes for

continuum assumption to be valid should not be below 3 mm [18]. The control volumes used in the present work are thus of the smallest permissible size. The maximum permissible time step for the stability of the heat Eq. (1) when solved using explicit scheme is compared with time scale of Eq. (2). If the time step for heat transfer equation is smaller, it is used for the calculation of both equations. If the time step for pyrolysis reaction is smaller, the time steps are chosen such that the heat transfer time step is an integer multiple of the reaction time step. Then, Eq. (2) is required to be advanced by that many time steps for each time step of Eq. (1).

Eq. (1) is discretized by integrating it over finite control volumes, to obtain a system of algebraic equations corresponding to each grid point in the domain. These algebraic equations are solved using the Alternating Direction Implicit method to advance in time. Making use of the temperatures thus computed, Eq. (2) is advanced in time using a fourth order Runge–Kutta method at each grid point in the domain until it reaches the same time level as Eq. (1). The change in density of the control volume is then used to compute the mass loss from the control volume in the current time step. From the proximate analysis presented in Table 1 the relative proportions of the various constituents is known, and hence the volumetric fractions of the remaining sawdust, char and void can be computed. The properties of the control volume, viz., its effective thermal conductivity and specific heat are then recomputed using Eqs. (4), (5a), (5b), (5c) and (6) at each time step, as described in Section 2.4. The total mass loss from the bed at each time step is the sum of the mass losses in all the grid control volumes in the domain in that time step. The cumulative sum of mass losses at all time steps until a given time t can thus be evaluated, and this can be compared with the experimental data.

In Eq. (1), ρ, C_p and k for sawdust and char, and in Eq. (2), the reaction rate k_r which is a function of temperature, and ρ_∞, need to be specified in order to make the model complete. Density of unpyrolysed sawdust for any packing density can be obtained by direct measurement of the mass and volume of the bed. Specific heat of sawdust and char can directly be used from literature, as stated above. The value of thermal conductivity, which is a function of packing density and the species of wood, needs to be obtained experimentally for the species of wood used in the present work at the packing density of interest. Similarly, the reaction rate k_r also depends on the species of wood and temperature, if we neglect autocatalysis effects due to residence of volatiles in the sawdust bed. The variation of k_r with temperature needs to be obtained for the species of wood. Also, the terminal value of density at the end of pyrolysis, ρ_∞, needs to be obtained by proximate analysis. In addition, one also needs experimental data to validate the model so developed. Hence, as part of the present work, experiments were carried out:

1) to estimate the thermal conductivity of sawdust (k_{sd}).
2) to obtain the variation of the reaction rate k_r with temperature, and the final density ρ_∞ of pyrolysed sawdust.
3) to pyrolyse sawdust in an annular bed, and to corroborate the predicted values of mass loss with the measured values.

Sawdust from a single lot obtained from the carpentry unit of IIT Delhi was sifted to obtain a uniform particle size in the range of 1–2 mm. Samples were taken from this lot for all the experiments mentioned above.

2.6. Boundary conditions

The heater wall temperature history measured from the experiments was used as boundary condition for the simulations. A convective heat loss with a heat transfer coefficient of 10 W m^{-2} K^{-1} was used as the boundary condition at the outer shell and the top surface of the sawdust bed. The base of the sawdust bed was assumed to be adiabatic. The bed was taken to be at ambient temperature at the beginning of the simulation. In mathematical terms,

Initial Conditions:

– $T\,(t = 0) = T_{amb}$ at all r, z for Eq. (1)
– $\rho = \rho_{sd}$ at all r, z for Eq. (2)

Boundary conditions of Eq. (1):

– Inner surface $r = r_i$: $T = T_w(z, t)$ from Fig. 5
– Outer surface $r = r_o$: $-k\partial T/\partial r = U(T - T_{amb})$ with $U = 10$ W m^{-2} K^{-1}
– Top surface $z = z_{max}$: $-k\partial T/\partial z = U(T - T_{amb})$ with $U = 10$ W m^{-2} K^{-1}
– Base surface $z = 0$: $\partial T/\partial z = 0$

3. Experimental estimation of parameters

This section describes in detail the various experiments carried out as part of the present work to estimate the necessary parameters listed above. Experiments for the estimation of thermal conductivity of the sawdust bed are described first. Subsequently, the experiments for the determination of reaction rates and final density of pyrolysed bed are detailed.

3.1. Thermal conductivity of sawdust bed

Sawdust particles packed in an annular bed can be approximated to be a homogeneous and isotropic porous medium, so long as the packing is uniform. Conduction of heat through porous media of this kind is difficult to model or predict in detail, given the tortuous path the flux lines need to take. The thermal conductivity of sawdust particles and that of the void need to be separately accounted for. It is difficult to measure f_{sd}, f_{ch}, k_{sd} or k_{ch} independently, although it is desirable since Eq. (4) models the effect of packing density on the conductivity of the bed. Instead, in the present work, it is attempted to estimate the thermal conductivity k of the sawdust bed directly, in a geometry as shown in Fig. 1b. The advantage of this approach is that sawdust can be rammed and packed in the same fashion as in a sawdust stove in the experimental rig as well, so that its packing densities are similar to that used in a sawdust stove. The difficulty with the approach is that it poses a parameter estimation problem, which is solved by trial and error in the present case.

The rig used for thermal conductivity estimation is shown schematically in Fig. 2. It is made up of a cylindrical electric heater enclosed in a metallic pipe of 40 mm outer diameter, 450 mm long. The heater is mounted vertically using a flange attached to one of the ends, to a circular wooden base, 240 mm in diameter. An outer cylindrical shell, 120 mm in diameter and 450 mm long, made up of a 1 mm thick sheet of mild steel, is mounted co-axially

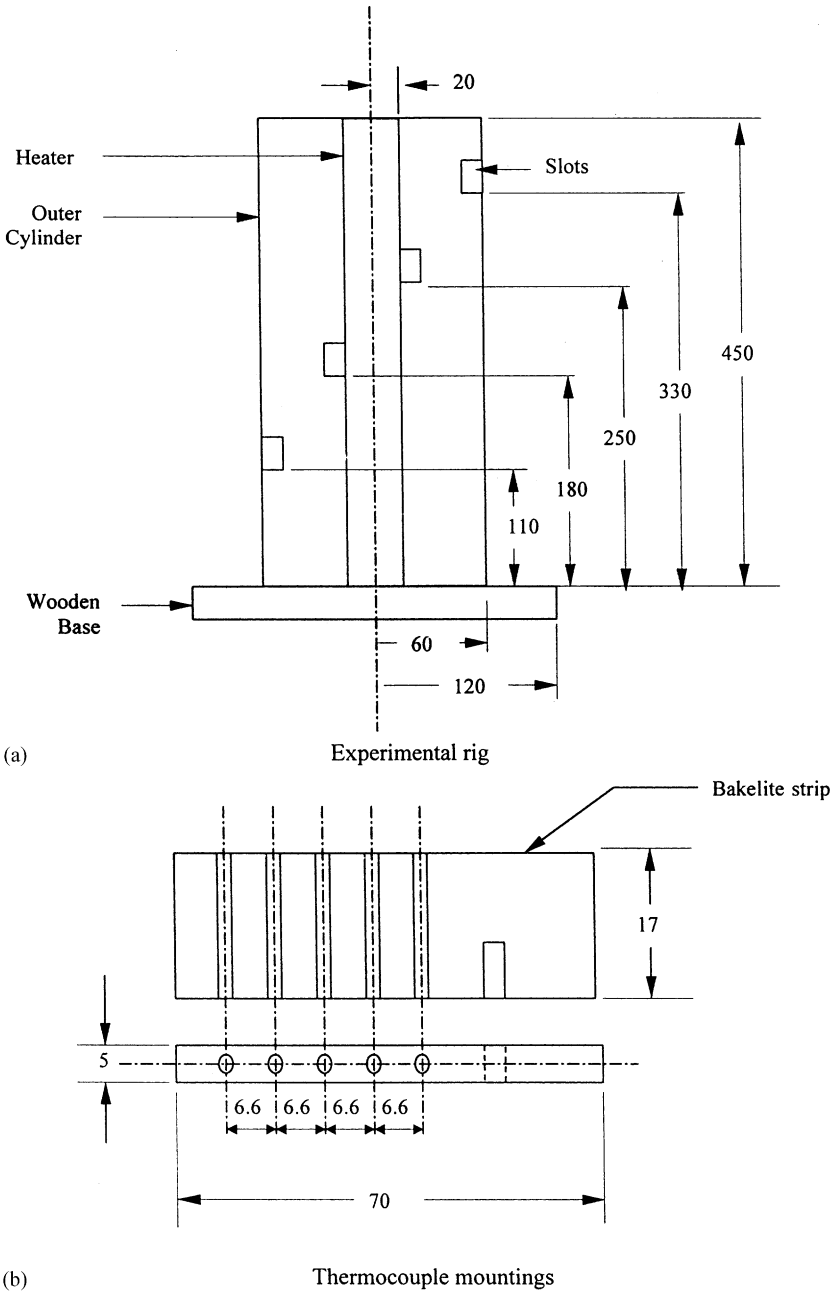

Fig. 2. Schematic of thermal conductivity experimental rig.

with the heater to the same wooden base. There is an annular space of 40 mm between the cylindrical heater and the outer shell, which is filled and packed with the sawdust sample whose thermal conductivity is to be estimated.

Temperature of the heater wall is measured at uniformly spaced points along the length of the cylinder, using Chromel–Alumel thermocouples fused into the metallic wall of the heater by silver filling. Also, temperature profiles in the annular region are measured at different heights using five thermocouples at each height, mounted using a bakelite strip. The bakelite strip ensures the correct positioning of the thermocouple junction beads in the bed. The bed is heated by the electric heater such that the temperature in the bed does not exceed 200 °C, so as to ensure that pyrolysis of the bed does not take place. The steady-state temperature profiles in the bed as well as on the heater wall were recorded for 10, 15 and 20 W electric power supplied to the heater. Since the total heat input to the sawdust bed $\dot{Q}_{\text{heater}}$ is known, we can estimate the flux distribution along the length of the heater. This is done by assuming that the sum of the thermal resistances offered by the contact resistance between heater wall and sawdust bed, the sawdust bed, the outer shell and the convective boundary layer outside outer shell is uniform along the height of the bed. Further, since the heater was fully buried in sawdust, the heat loss from the top surface of the heater can be neglected. It was also observed that since the heating element occupies the central portion of the heater, the ends of the heater are at a lower temperature than its central portion. Hence, the temperature distribution in the sawdust bed is two-dimensional. However, since the axial temperature gradients in the sawdust bed are small compared to the radial gradients, we could neglect the axial conduction, rendering the analysis one-dimensional. In the present work, since temperatures are measured along the length of the heater, the heater could be divided into segments of uniform temperature, with equal thermal resistance R_{th} in the radial direction. Then, along the length of the heater,

$$\sum_{\text{i}} \frac{T_{\text{wi}} - T_{\text{amb}}}{R_{\text{th}}} A_{\text{i}} = \dot{Q}_{\text{heater}} \tag{7}$$

where T_{wi} is the temperature of the heater wall in segment i, A_{i} is the area of segment i and T_{amb} and R_{th} are the ambient temperature and the total thermal resistance, respectively. All other terms than R_{th} in Eq. (7) are known, and hence it can be computed. Using this R_{th}, the heat flux values for any segment of the sawdust bed can be computed as

$$\frac{T_{\text{wi}} - T_{\text{amb}}}{R_{\text{th}}} A_{\text{i}} = \dot{Q}_{\text{i}} \tag{8}$$

Since $q_{\text{i}} = \dot{Q}_{\text{i}}/A_{\text{i}}$ is also equal to the flux across the sawdust bed, we can relate q_{i} to the thermal conductivity of the bed assuming steady state one-dimensional conduction as follows:

$$q_{\text{i}} = -k_{\text{sd,moist}} \left.\frac{\partial T}{\partial r}\right|_{r_{\text{h}}} = -k_{\text{sd,moist}} \frac{(T_1 - T_2)}{r_{\text{h}} \ln \frac{r_1}{r_2}} \tag{9}$$

Here, T_1 and T_2 are the temperatures measured at radii r_1 and r_2, respectively, in the sawdust bed and r_{h} is the radius of the heater. Since the central portion of the experimental bed had the smallest magnitude of axial temperature gradients heat transfer is more nearly

Table 3
Thermal conductivity of sawdust with moisture

Wattage	10 W	15 W	20 W	Mean
$k_{sd,moist}$ (W m^{-1} K^{-1})	0.059	0.056	0.066	0.0603

one-dimensional in this portion. Hence, the segment of the sawdust bed in this portion was used in the one-dimensional Eq. (9) to obtain $k_{sd,moist}$. Table 3 presents the values of $k_{sd,moist}$ of sawdust bed obtained for different values of heater wattages. Since this sample of sawdust is known to contain 7.9% moisture and 92.1% dry sawdust, knowing their respective densities, the volumetric fractions of sawdust and water are computed. Then, using Eq. (4) for $k_{sd,moist}$ as a function of thermal conductivity of dry sawdust, k_{sd} and that of liquid water, k_w, thermal conductivity of dry sawdust, k_{sd}, can be calculated.These values are in close agreement with those obtained from Touloukian and Ho [20], who give a thermal conductivity of 0.065 W m^{-1} K^{-1} at 24 °C for sawdust. It also agrees well with the expression of Ten Wolde et al. [23]:

$$k_{sd} = S(0.1941 + 0.4064M) + 0.01864 \text{ W m}^{-1}\text{ K}^{-1}$$

which gives a value of 0.07 W m^{-1} K^{-1} for specific gravity $S = 0.23$ and moisture mass fraction $M = 0.079$, the data for the present sample of sawdust.

3.2. Reaction rate constant and final density

The present model assumes that the pyrolysis rate is not affected by the autocatalysis due to the residence of the products of pyrolysis. In such a case, the rate of mass loss at any temperature, for a given heating rate, can be directly obtained from the TGA of the sawdust sample. In TGA, a small sample of the fuel to be studied is placed on a micro balance, and heated at a specified rate of temperature rise, in a specified atmosphere, simultaneously recording temperature and the mass of the sample. In the present work, TGA of sawdust was carried out at 10 and 100 °C min^{-1} in an atmosphere of nitrogen. Using Eq. (2), we can then obtain the value of k_r as a function of temperature by the following expression:

$$k_r = \frac{-\mathrm{d}\rho/\mathrm{d}t}{(\rho - \rho_\infty)} = \frac{-\mathrm{d}m/\mathrm{d}t}{(m - m_\infty)} \tag{10}$$

With the assumption that no shrinkage of volume occurs due to pyrolysis, the mass remaining after pyrolysis would determine the final density. Proximate analysis of the sawdust gives its contents of moisture, volatiles, fixed carbon and ash. The fraction of moisture and volatiles escape during pyrolysis and the fractions of fixed carbon and ash remain. This final mass of sawdust divided by the total volume, which is assumed invariant, gives the final density ρ_∞ of pyrolysed sawdust bed. Table 1 presents the proximate analysis of the sawdust sample obtained from experiments. The final density ρ_∞ is taken to be 21.9% of the initial density, i.e., the sum of ash and fixed carbon fractions of the bed. Using this in Eq. (10), we can obtain the reaction rate constant k_r at each temperature. Fig. 3a shows the variation of k_r with temperature obtained from TGA on a sample of the sawdust at 10 °C min^{-1} in an atmosphere of nitrogen.

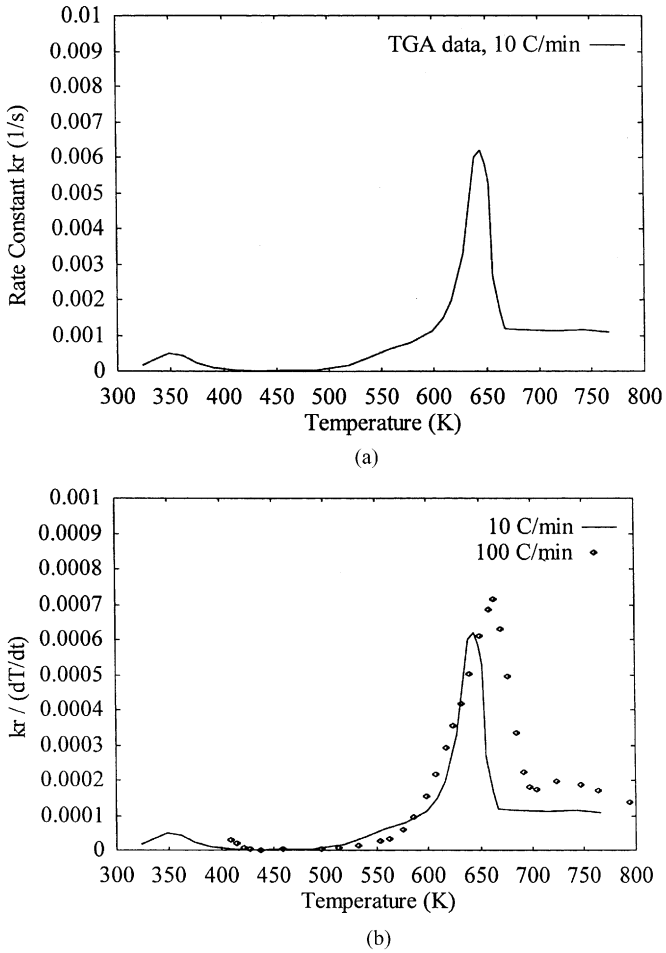

Fig. 3. Reaction rate of pyrolysis from TGA, (a) Reaction rate constant derived from TGA at 10 °C min^{-1}, (b) Scaling of reaction rate constants by heating rate.

Since the rate constant of pyrolysis k_r is a strong function of the heating rate, it would be inappropriate to use the TGA data obtained for a heating rate of 10 °C min^{-1} for all the heating rates encountered during pyrolysis of the sawdust bed. In order to account for the variation of k_r with the heating rate dT/dt, the value of k_r/(dT/dt) obtained from TGA for two heating rates, viz., 10 and 100 °C min^{-1} in nitrogen were plotted together, as shown in Fig. 3b. It can be seen that the two curves are not only qualitatively similar, but also almost collapse onto one another. This shows that k_r variation with temperature is scalable by the heating rate with minimal error, in the range investigated. In the present work, the value of dT/dt is computed for each control volume in each time step, and the corresponding k_r value is evaluated using the following expression:

$$k_r = k_{r,\mathrm{TGA}} \frac{(\mathrm{d}T/\mathrm{d}t)}{(\mathrm{d}T/\mathrm{d}t)_{\mathrm{TGA}}} \tag{11}$$

where $\mathrm{d}T/\mathrm{d}t$ is the heating rate for a control volume at any instant, while $(\mathrm{d}T/\mathrm{d}t)_{\mathrm{TGA}}$ corresponds to the heating rate under which the TGA data were obtained. TGA data obtained at $10\,^{\circ}\mathrm{C\ min}^{-1}$ has been used as the reference input for all the simulations carried out in the present work.

4. Pyrolysis of sawdust bed

4.1. Experimental rig

As described in the preceding sections, the aim of the present work is to develop a model for computational simulation of pyrolysis of an annular sawdust bed, conduct experiments of pyrolysis in a sawdust bed and validate the model against the experimental results. To achieve this goal, an experimental rig was designed to pyrolyse an annular sawdust bed and measure the mass loss as a function of time, while monitoring the temperatures on the heater wall and in the annular bed being pyrolysed. The geometry used in this rig is quite similar to the one used in the experiments for estimation of thermal conductivity described in Section 3.1. The schematic of the rig is shown in Fig. 4. It comprises a heater whose diameter is 32 mm and height is 300 mm, mounted vertically on an asbestos base sheet using a flange. Seven equally spaced Chromel–Alumel thermocouples are fixed on the heater wall to monitor the temperatures. These thermocouples are fixed into 2 mm diameter holes on the heater walls using silver filling. Asbestos mountings were used in the same manner as the bakelite mountings shown in Fig. 2, so as to sustain the temperatures

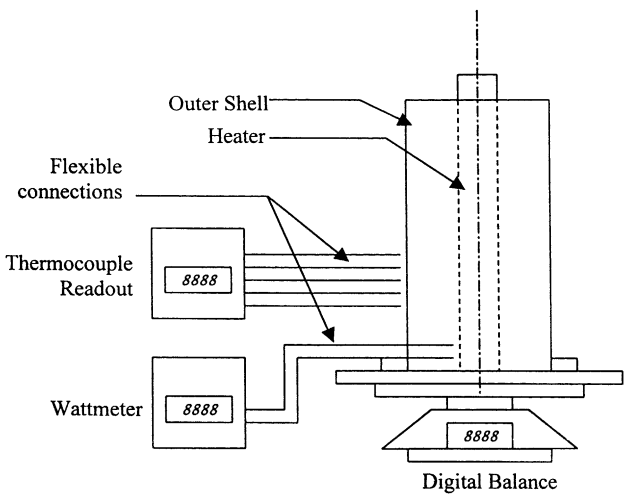

Fig. 4. Schematic of the pyrolysis experimental rig.

in the pyrolysis zone. These mountings support seven thermocouples each, at fixed radial locations. The thermocouples are glass wool-insulated Chromel–Alumel junctions, inserted through 2 mm diameter holes drilled through the 6 mm thick asbestos mounting strips. The thermocouple mountings are fixed to an outer cylindrical shell whose inner diameter is 132 mm and length is 300 mm. Six slots are cut on this shell at equal axial distances, 60 mm apart from each other, to accommodate the thermocouple mountings. These mountings are arranged around the periphery of the shell circumferentially staggered from each other for convenience in ramming sawdust and to prevent any bias. Thus, temperatures at 42 different locations in the sawdust bed can be monitored. The rig is mounted on an asbestos base plate and placed on a digital top-loading balance to measure mass loss. The balance has a range of 0–13 kg with a resolution of 1 g. The heater is connected to the electric mains through an autotransformer to regulate its wattage. The power supplied to the heater is monitored using a digital wattmeter of range 0–999 W with a resolution of 1 W. The uncertainty in the mass measurements introduced by the thermocouple connections was maintained less than ± 1 g at any point of time, by rigidly supporting the thermocouple wires on a stand. This was confirmed several times during the course of each experiment by placing and removing standard masses ranging from 1 to 50 g and checking the readings of the digital balance every time for hysteresis effects. It was observed that the hysteresis effects were low enough to repeatably read the addition and removal of even a 1 g mass. Experiments were conducted at a heater wattage of 150 W, and the mass loss from the sawdust bed was recorded over a period of 2 h with simultaneous recording of the temperatures. Fig. 5 shows the temperature profiles at various times as recorded from the experiment.

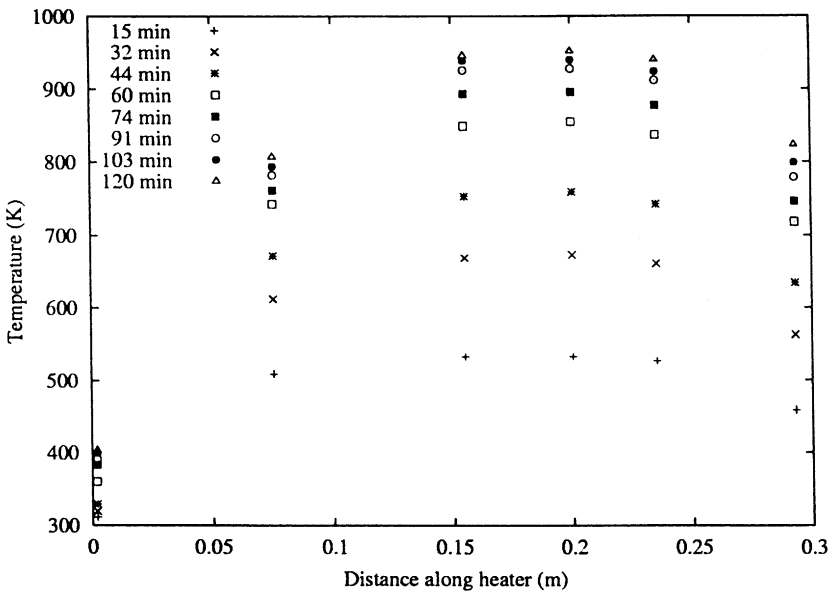

Fig. 5. Measured temperature profiles along the heater wall.

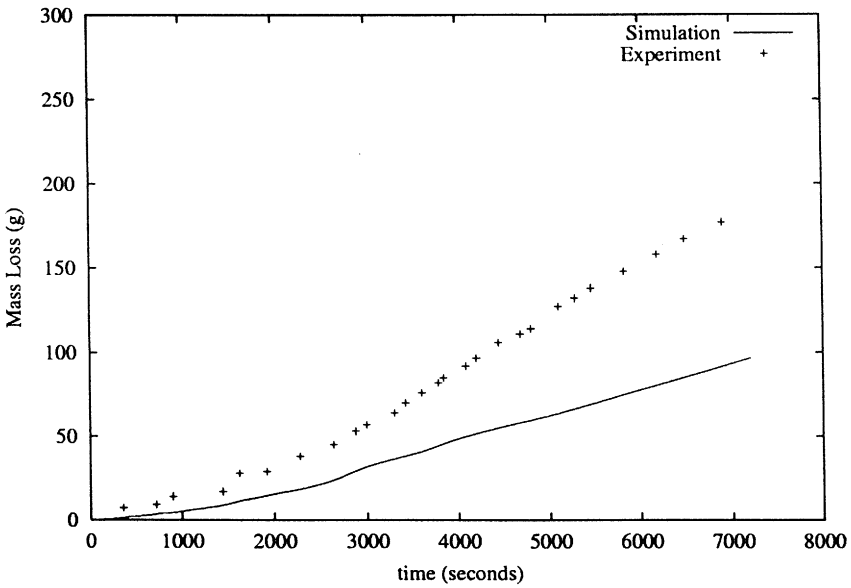

Fig. 6. Comparison of predicted baseline mass loss history with experiment.

4.2. Comparison of simulation with experiment

The model for pyrolysis discussed in Section 2 has been coded in a FORTRAN program. This program was run to simulate the experiment described in Section 4.1. The temperature profiles along the length of the heater measured from the experiment at different times, as shown in Fig. 5 have been used as boundary conditions in the simulation program. The physical properties of sawdust and char listed in Table 2 and the reaction rate constants obtained from TGA have been used. The terminal density of the bed at the end of pyrolysis was taken according to the (char + ash) fraction of the sawdust specimen presented in Table 1. The predicted mass loss history is shown in Fig. 6, alongside the measured mass loss history from the experiment. At a first glance, there is qualitative agreement in the trends of experimental and predicted mass loss histories. But the slope of the mass loss curve, i.e., the rate of mass loss, is distinctly higher in the experimental data as compared to the predicted history. The cumulative mass loss at the end of 2 h is 177 g in the experiment, while the prediction is much lower at 96.8 g.

The possible reasons for the discrepancy could be listed as follows:

1) Uncertainty in property data used for the simulation.
2) Effect of flow of volatiles inside the sawdust bed on the heat transfer, which is not accounted for in the present model.
3) Effect of residence of volatiles inside the sawdust bed, and the secondary pyrolysis that ensues, on the reaction rates.

A sensitivity analysis on the effect of these factors would throw better light on the phenomenon of pyrolysis and the factors to which the phenomenon is most sensitive.

4.3. Sensitivity analysis

In this section, the program developed in the present work is used to perform a sensitivity analysis of the predicted mass loss history to the aforementioned uncertainties. This exercise should bring out effects of these uncertainties, and the precautions to be taken while conducting studies on the pyrolysis of sawdust.

The property data used for simulation pertains to the values of density, thermal conductivity and specific heat values of the constituents of the sawdust bed, viz., sawdust, moisture, char and void. Out of these, density and thermal conductivity of sawdust in the temperature range encountered by sawdust in the pyrolysis experiment have been determined by experiments on the same specimen. Specific heat data for wood and sawdust have been comprehensively documented in literature as a function of moisture content and specific gravity [21]. For the solid part of char, Ragland et al. [21] recommend that properties of graphite can be used. Since graphite is anisotropic, the thermal conductivity along and across the grains of graphite are very widely different: while the conductivity along the grains is 790 W m^{-1} K^{-1} at 600 K, that perpendicular to the grains is as low as 2.68 W m^{-1} K^{-1}. The properties of void used in the present work are relatively tentative: void is assumed to have the thermal conductivity equal to that of air at 600 K. This assumption was necessary since thermal conductivity of volatile matter is not available from literature.

Besides, the heat transfer in the void region of char bed is also likely to be enhanced by flow of volatiles in this region. Secondary pyrolysis could increase the reaction rate of pyrolysis. Since TGA data have been obtained from small samples of sawdust, this effect is not accounted for in the present model.

Hence, in this section, the sensitivity of the predicted mass loss history to three parameters is examined: thermal conductivity of solid char; thermal conductivity of void; and the reaction rate constant. In order to study the effect of rate constant, a reaction rate multiplier has been used. The reaction rate calculated for any control volume using Eq. (11) is multiplied by this multiplier to redefine its value for parametric analysis. For parametric study, all parameters and properties are held constant other than the parameter being investigated.

4.3.1. Effect of thermal conductivity of char

Fig. 7 shows the effect of thermal conductivity of solid char k_{ch}. It can be expected that an increase in k_{ch} improves the rate of heat transfer to the pyrolysis front, and hence enhances pyrolysis rate. This is clearly reflected in Fig. 7. However, since the density of solid particles of char is much higher than the density of sawdust, the void fraction in the pyrolysed bed is high, and thus, any change in the thermal conductivity of solid char does not have a pronounced effect on the mass loss predictions. Even for an increase in k_{ch} by three orders of magnitude, the cumulative mass loss due to pyrolysis at the end of 2 h increases only by about 15%. This indicates that an uncertainty in the thermal conductivity of char could not have resulted in the discrepancy observed between the experimental data and predictions shown in Fig. 6.

4.3.2. Effect of thermal conductivity of void

Fig. 8 shows the effect of thermal conductivity of the void space in the char bed on the mass loss predictions. Since the completely pyrolysed bed contains mostly void and less

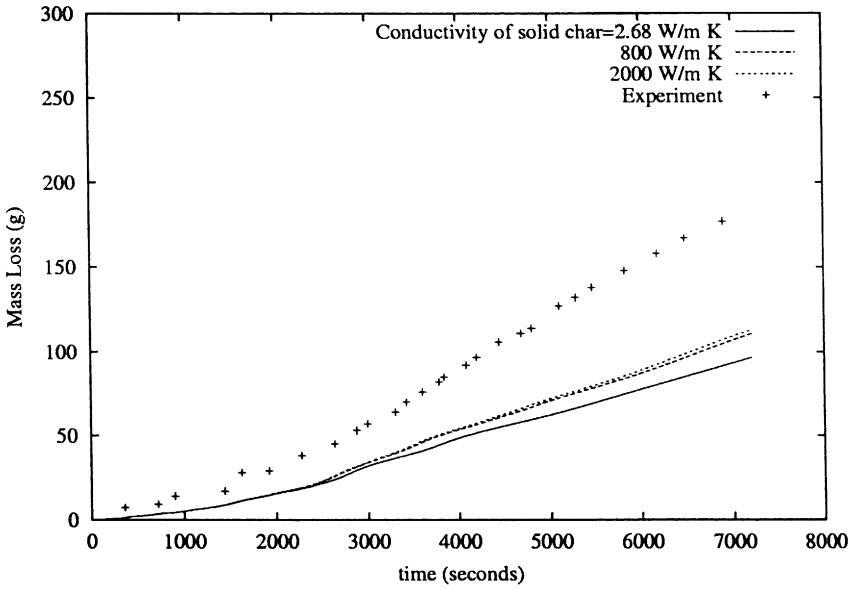

Fig. 7. Effect of thermal conductivity of solid char on predicted mass loss history.

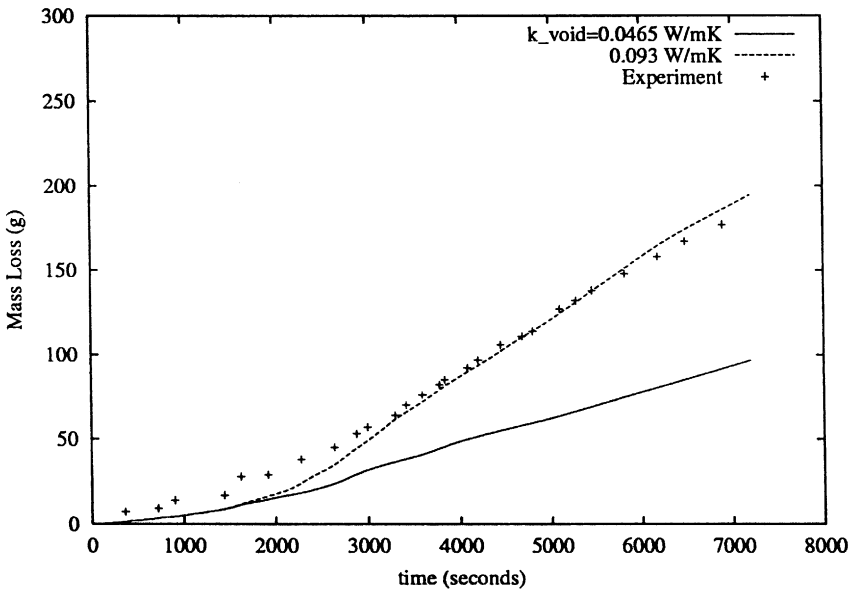

Fig. 8. Effect of thermal conductivity of void on predicted mass loss history.

char in volume, thermal conductivity of void plays a critical role in determining the rate of heat supply to the pyrolysis front from the heater. Fig. 8 shows this clearly: a higher value of thermal conductivity of void results in a higher rate and magnitude of mass loss predicted by the model. Better still, a twofold increase in the thermal conductivity of void results in a very close agreement between the predicted mass loss curve and the experimental mass loss curve. For a k_{void} value of $0.093 Wm^{-1}k^{-1}$, which is twice the baseline value of $0.0465 Wm^{-1}k^{-1}$, we observe that the slope of the mass loss curve predicted is higher than that of the experimental curve, indicating an overprediction of the rate of mass loss. It is also observed that in the initial phase, i.e., until about 3000 s of pyrolysis, the predicted mass loss is well below the experimental data for both values of k_{void}. These observations show that during the latter phase of pyrolysis, where the porosity of the bulk of the bed is high, a higher value of k_{void} can help the simulated data match the slope of the experimental data. In other words, the enhancement of heat transfer due to flow of volatiles in the void region causes a discrepancy of predictions with experiment. This discrepancy decreases if one assumes a higher transfer rate due to artificially marked-up thermal conductivity of void.

4.3.3. Effect of reaction rate constant

In order to study the effect of the reaction rate k_r of pyrolysis, a multiplier was artificially introduced into the simulation program. A unit value of the multiplier means that the values of k_r, as calculated using Eq. (11), are used. Simulations were carried out for values 0.5, 5 and 10 of the multiplier, which mean that the reaction rate was 50% less, 5 and 10 times higher than the values obtained using Eq. (11) at any temperature, respectively in the three cases. Fig. 9 compares the mass loss histories for these cases. It is observed from the figure that there is a significant decrease in mass loss rate with a decrease in reaction rate at all

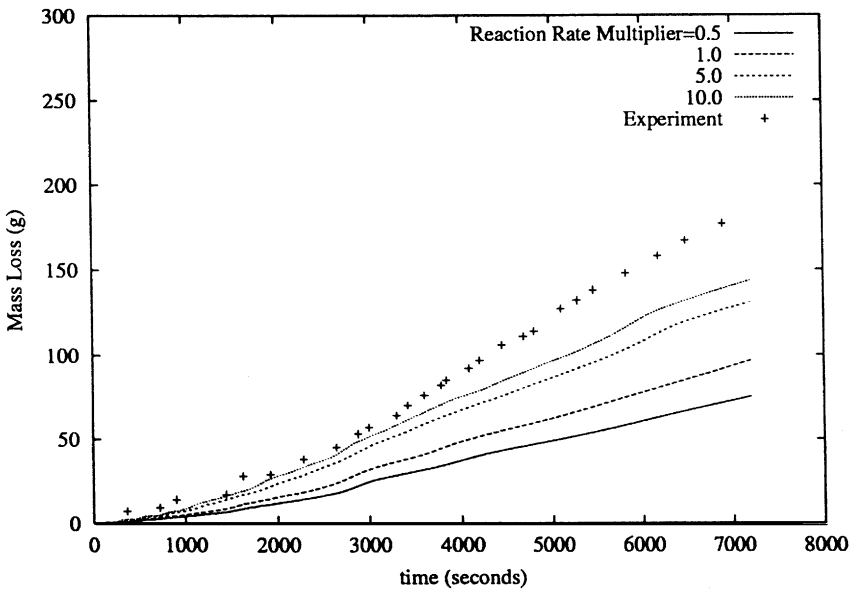

Fig. 9. Effect of pyrolysis reaction rate on predicted mass loss history.

times from the beginning of pyrolysis until the end of 2 h. The converse effect is also visible clearly in Fig. 9. It can be observed that, while even a tenfold increase in the reaction rates does not help the simulation to match the mass loss rate of the experiment, the agreement in the initial period of pyrolysis (upto 3000 s) is much better with a higher reaction rate multiplier. This indicates that when the porosity of the bed is low, the residence of the volatiles in the bed results in a higher reaction rate, which causes the discrepancy between the experiments and simulation in this period. This is rectified when one artificially assumes a higher reaction rate during this period, as is shown in Fig. 9.

4.4. Discussion

It becomes amply clear from the foregoing sensitivity analysis that the uncertainties in property data do not seem to have a pronounced effect on the predictions, and hence, the baseline values of properties listed in Table 2 are adequate for the simulations. The discrepancy between the experiments and simulations, as is demonstrated by the sensitivity analysis, is because the simulation does not account for two phenomena: flow of volatiles in the void space of the char bed, and secondary pyrolysis due to residence of volatiles, especially in the early part of pyrolysis.

A simulation was carried out with a reaction rate multiplier value of 8 and k_{void} of 0.06, combining the observations from the sensitivity analysis. The comparison of predictions using these corrections to the baseline data with experimental results is shown in Fig. 10. It is seen that the agreement of this prediction with experimental data is very good over practically the entire time range, thus supporting the above discussion.

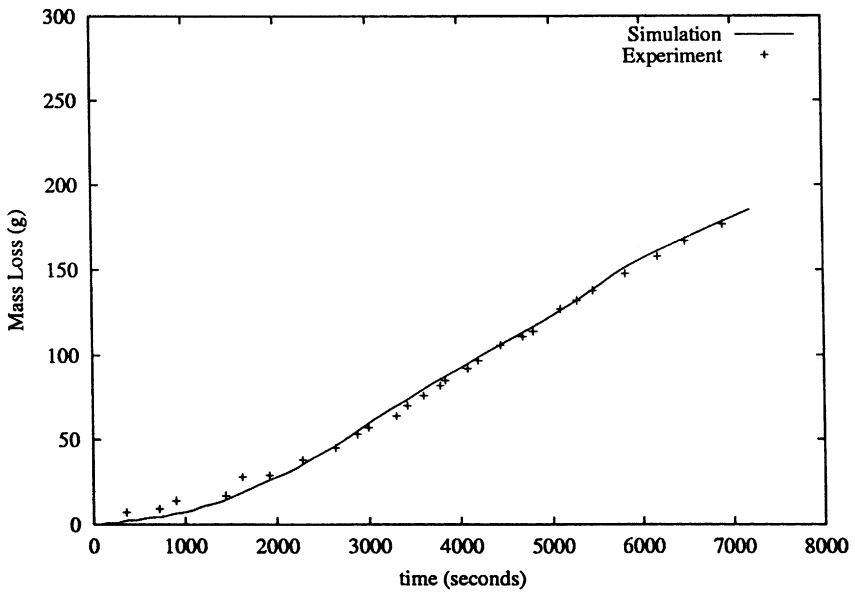

Fig. 10. Predicted mass loss history with revised property data.

5. Conclusions

This article presents the development of a semi-empirical model for pyrolysis of sawdust in an annular packed bed. Experimental measurements and estimation have been used to obtain data that cannot be obtained from literature with certainty. Thermal conductivity of the sawdust bed and the apparent kinetic reaction rates of the pyrolysis reaction have been obtained for the sample of sawdust on which pyrolysis experiments have been performed. The simulation model developed on the basis of these data has been compared with pyrolysis experiments performed in the present work. The results show that the model underpredicts the values of mass loss and mass loss rates. A sensitivity analysis using the model suggests that the predictions may be improved by considering the flow of volatiles in the void space of char bed, and by accounting for secondary pyrolysis due to residence of volatiles in the bed.

References

[1] C.A. Zaror, D.L. Pyle, K. Krishna Prasad, P. Verhaart (Eds.), Wood Heat for Cooking, Indian Academy of Sciences, Bangalore, 1983, p. 15.
[2] C.H. Bamford, J. Crank, D.H. Malon, Proc. Camb. Philol. Soc. 42 (1946) 166.
[3] H.C. Kung, Combust. Flame 18 (1972) 185.
[4] T. Matsumoto, T. Fujiwara, J. Kondo, Twelfth Symposium (International) on Combustion, The Combustion Institute, Pittsburgh, 1969, p. 515.
[5] P.S. Maa, R.C. Bailie, Combust. Sci. Technol. 7 (1973) 257.
[6] A.F. Roberts, Sixteenth Symposium (International) on Combustion, The Combustion Institute, Pittsburgh, 1971, p. 893.
[7] E.J. Kansa, H.E. Perlee, R.F. Chaiken, Combust. Flame 29 (1977) 311.
[8] W.C.R. Chan, M. Kelbon, B. Krieger, Fuel 64 (1985) 1505.
[9] E.R. Tinney, Tenth Symposium (International) on Combustion, The Combustion Institute, Pittsburgh, 1965, p. 925.
[10] C.A. Koufopanos, N. Papayannakos, G. Maschio, A. Lucchesi, Can. J. Chem. Eng. 69 (1991) 907.
[11] C.K. Lee, R.F. Chaiken, J.M. Singer, Sixteenth Symposium (International) on Combustion, Combustion Institute, Pittsburgh, 1976, p. 1459.
[12] C. Di Blasi, Int. J. Heat Mass. Tran. 41 (1998) 4139.
[13] C. Di Blasi, Prog. Energ. Combust. Sci. 19 (1993) 71.
[14] S. Sinha, A. Jhalani, M.R. Ravi, A. Ray, SESI J. 10 (1) (2000) 41.
[15] F. Shafizadeh, J. Anal. App. Pyrol. 3 (1982) 283.
[16] H.W. Emmons, A. Atreya, in: K. Krishna Prasad, P. Verhaart (Eds.), Wood Heat for Cooking, Indian Academy of Sciences, Bangalore, 1983, p. 5.
[17] R. Bilbao, J.F. Mastral, M.E. Aldea, J. Ceamanos, J. Anal. App. Pyrol. 36 (1996) 81.
[18] M. Kaviany, Principles of Heat Transfer in Porous Media, Springer, New York, 1991, p. 8.
[19] A. Bejan, D.A. Nield, Convection in Porous Media, Springer, New York, 1992.
[20] Y.S. Touloukian, C.Y. Ho (Eds.), Thermophysical Properties of Matter, Plenum Press, New York, 1972.
[21] K.W. Ragland, D.J. Aerts, A.J. Baker, Bioresource Technol. 37 (1991) 161.
[22] A.T.D. Butland, R.J. Maddison, J. Nucl. Mater. 49 (1973) 45.
[23] A. Ten Wolde, J.D. Mc Natt, L. Krahn, DOE/USDA-21697/1, Oak Ridge National Laboratory, Oak Ridge, TN, 1988.